Available online at www.sciencedirect.com
ScienceDirect
Electrochimica Acta 53 (2008) 4907–4919
ELECTROCHIMICA Acta
www.elsevier.com/locate/electacta

Metallo-functionalized first-generation salicylaldimine poly(propylenimine) tetraamine dendrimers: Electrochemical study and atomic force microscopy imaging

Jasmina Martinovic [a,b], Ana-Maria Chiorcea-Paquim [a], Victor Constantin Diculescu [a], Juanita Van Wyk [b], Emmanuel Iwuoha [b], Priscilla Baker [b], Selwyn Mapolie [b], Ana-Maria Oliveira-Brett [a,*]

[a] *Departamento de Química, Faculdade de Ciências e Tecnologia, Universidade de Coimbra, 3004-535 Coimbra, Portugal*
[b] *Chemistry Department, University of the Western Cape, Private Bag X17, Bellville 7535, South Africa*

Received 14 December 2007; received in revised form 25 January 2008; accepted 1 February 2008
Available online 13 February 2008

Abstract

The adsorption and the redox processes of two first-generation salicylaldiamine dendritic ligands and their copper, cobalt and nickel metallo-functionalized complexes have been studied at two types of carbon electrode surface. Glassy carbon (GC) was used in an electrochemistry study and highly oriented pyrolitic graphite (HOPG) in *ex situ* atomic force microscopy (AFM) imaging. All salicylaldimine ligands and their metallo-functionalized complexes adsorb on the surface of the HOPG electrode, resulting in the formation of nanoclusters and films, which vary between 0.9 and 6 nm in size, depending on the metallo-functionalized salicylaldimine dendrimer chemical composition and solution concentration. Differential pulse voltammetry of the surface-confined films has shown that the anodic reactions observed correspond to the oxidation of the hydroxyl groups present in the ligand structure of all compounds. However, by following the changes in peak currents, potentials and width at half height it has been shown that destabilization of the ligand internal structure occurred in the metallo-functionalized complexes depending on the metal involved. The electrochemical behaviour of the surface-confined films observed in buffer solution was related to the morphology, obtained by AFM, of the immobilised first-generation salicylaldiamine dendritic ligands and corresponding salicylaldimine metallo-functionalized complexes.

Keywords: Dendrimers; Salicylaldimine metallo-functionalized complexes; Atomic force microscopy (AFM); Differential pulse voltammetry (DPV)

1. Introduction

Dendrimers represent a synthetic class of highly branched spherical polymers, formed using a nanoscale, multistep fabrication processes [1,2]. Dendrimers are highly branched and have a spherical structure formed by a central core, multiple peripheral reactive site end-groups, and branching units constituted of repeating units that link the core to the multiple peripheric reactive site end-groups. These peripheral reactive sites are modified with the desired end-groups or functionalities according to the proposed applications. The number of branching units between the core and reactive end-group is called the generation number and is determined by the number of synthetic cycles. Each step on adding a branched unit to the molecule results in a new "generation" of dendrimers that has twice the complexity of the previous generation, the generation number increasing by one, and first-generation dendrimer being the simplest one. This has the effect of amplifying the dendritic branching and generating new supramolecular dendrimers.

Due to their structural characteristics, dendrimers present new physical and chemical properties, when compared to linear polymers, dominated by the specific functional groups existent on their molecular surface employed in order to reach new and specific properties. Several applications of dendrimers reported in the literature are related to their biological and pharmaceutical properties [3].

Great progress was made in developing new metallodendrimers, which are of enormous interest due to their numerous

* Corresponding author. Tel.: +351 239 835295; fax: +351 239 835295.
E-mail address: brett@ci.uc.pt (A.-M. Oliveira-Brett).

0013-4686/$ – see front matter © 2008 Elsevier Ltd. All rights reserved.
doi:10.1016/j.electacta.2008.02.013

potential applications, such as the development of new materials, photochemistry, liquid crystals, artificial photosynthetic systems, molecular electronics, electrochemistry and catalysis [4,5]. Metallodendrimers with important electronic, magnetic and catalytic properties were reported in the literature [6] and various families of metallodendrimers have been used as macromolecular supports in catalysis [7]. Dendrimers were also used as encapsulating agents for insoluble materials [8,9], models for self-assembled monolayers, colloids or nanoclusters [3,10] as well as chemiresistors [6,11].

Electroactive dendrimers were shown to be very important candidates for use in practical applications such as electron-transfer mediators, energy converters, ion sensors or electronic devices [3,6,12–16]. Voltammetry enables the study of the surface-confined electroactive dendrimer films. It has been shown that the dendrimer can influence the microenvironment around the electroactive centers and these studies were focused on both the dendritic wedge effect on the electroactive center (core) and the redox behaviour of multiple electroactive sites on the higher generation dendrimer surfaces [3,12–18].

The structure, shape, size, solubility and catalytic activity of the metallodendrimers are directly influenced by the type of metal incorporated, by the specific location of the metal within the dendrimer structure, at the periphery or at the core, and by the specific dendrimer topology. The electrochemical properties of metallodendrimers are directly related to the number of metal-active functional groups incorporated in the dendrimer, which can be controlled. It was noted that low generation dendrimers, such 1 and 2, that present open and asymmetric structures, are more attractive metallodendrimers for catalysis purposes [4,19], in contrast with higher generation dendrimers. In general, slower rates of reaction were observed with increasing dendrimer generation and the recovery of the catalytic material was demonstrated to be more efficient with dendrimers of moderate sizes. Consequently the synthesis of new small metallodendrimers is relevant from the viewpoint of catalytic applications.

Electrochemistry provides information on electron transfer between electroactive moiety and electrode surface, where a decrease in the peak current, an increase in the potential, and a broadening of the voltammetric wave are related to the degree of the inhibition or electron transfer, and due to their high sensitivity, voltammetric methods have been successfully used to study the redox behaviour of dendrimer electrode surface modifiers [3,6,12–18].

Two different substituted salicylaldiamine dendritic ligands were employed in this study, ligand 1 (Lig1) and ligand 2 (Lig2) (Scheme 1). They were synthesized [7] starting with the commercially available poly(propylenimine) tetraamine dendrimer (DAB-dendr-$(NH_2)_4$), via the Schiff-base condensation reaction. The formation of first-generation metallo-functionalized

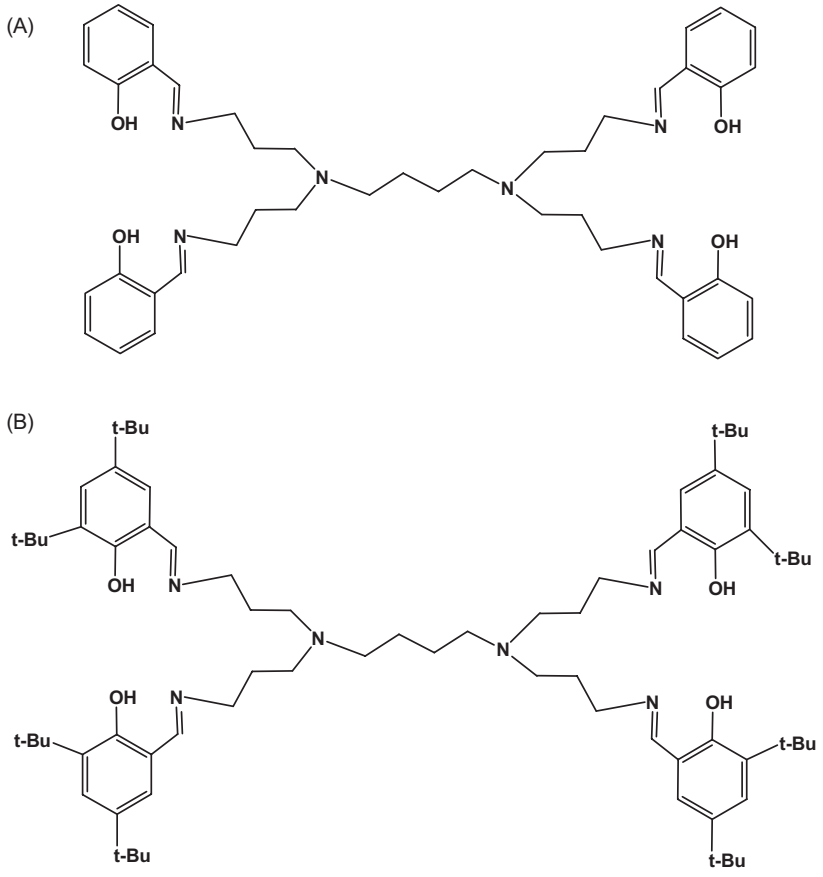

Scheme 1. First-generation salicylaldiamine dendrimer: (A) Lig1 and (B) Lig2.

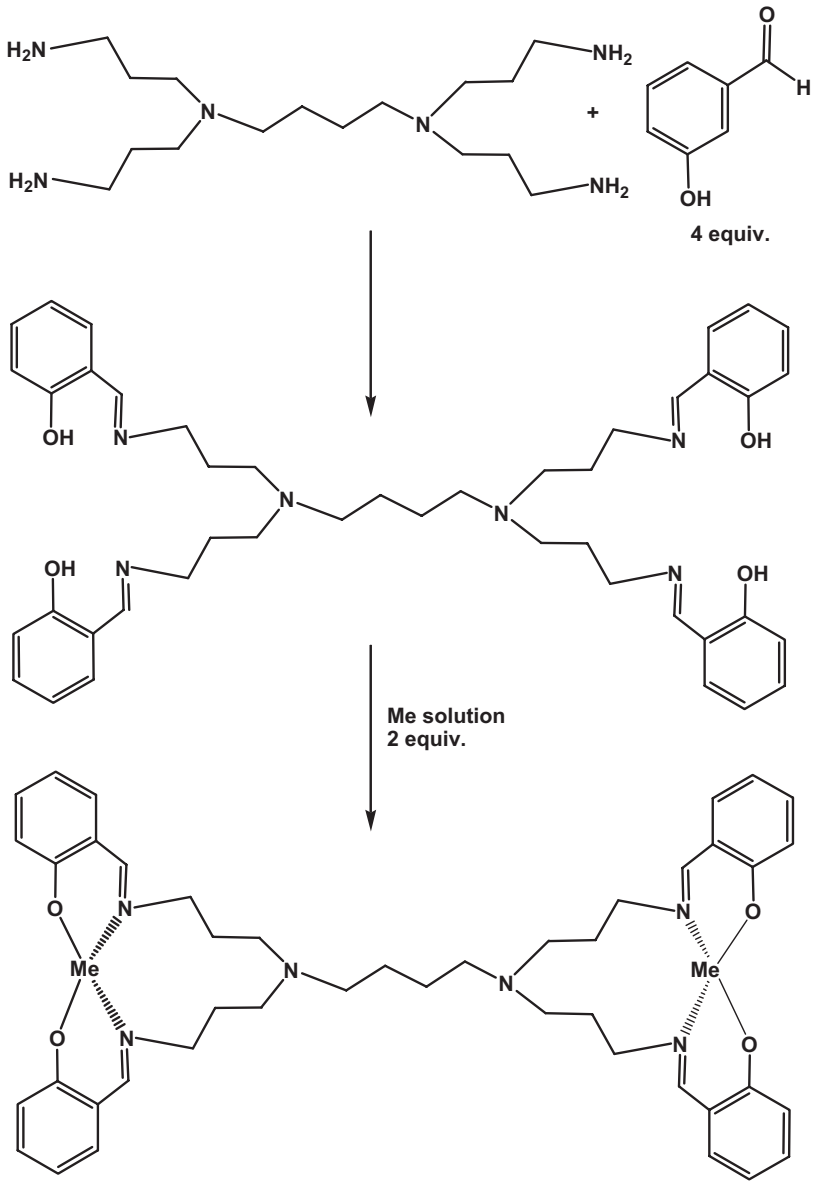

Scheme 2. Synthesis of first-generation salicylaldiamine Lig1 and metallo-functionalized salicylaldimine Lig1 dendrimers.

dendrimers of cobalt, copper and nickel complexes with salicylaldiamine ligand 1 (Co–Lig1, Cu–Lig1, and Ni–Lig1) and of cobalt and copper with salicylaldiamine ligand 2 (Co–Lig2, and Cu–Lig2) followed Scheme 2. The first four generations of salicylaldiamine poly(propylenimine) tetraamine dendrimer (DAB-dendr-$(NH_2)_x$) ($x = 4$, 8, 16 and 32), incorporating metals on the periphery of the dendritic structure, Scheme 3, are also being synthesized.

The present study focused on the electrochemical characterization and magnetic ac mode atomic force microscopy (MAC Mode AFM) imaging of two first-generation salicylaldiamine dendritic ligands and their copper, cobalt and nickel metallo-functionalized complexes adsorbed onto two different types of carbon electrode surface, highly oriented pyrolitic graphite (HOPG) and glassy carbon (GC). The nanosize resolution AFM images of adsorbed dendrimer films will clarify the surface assembling process at the molecular level, and the nature and strength of this first-generation synthetic cobalt, copper and nickel salicylaldiamine metallo-functionalized dendrimers on the carbon surfaces. Special attention was given to the deposition conditions of these small size salicylaldimine metal complexes on the surface of two different types of carbon electrode in order to characterize their electrochemical behaviour and surface morphology.

2. Experimental

2.1. Materials and reagents

All solutions were prepared using analytical grade reagents and purified water from a Millipore Milli-Q system (conductivity $\leq 0.1\ \mu S\ cm^{-1}$). Buffer solutions used as supporting electrolytes in the experiments are shown in Table 1.

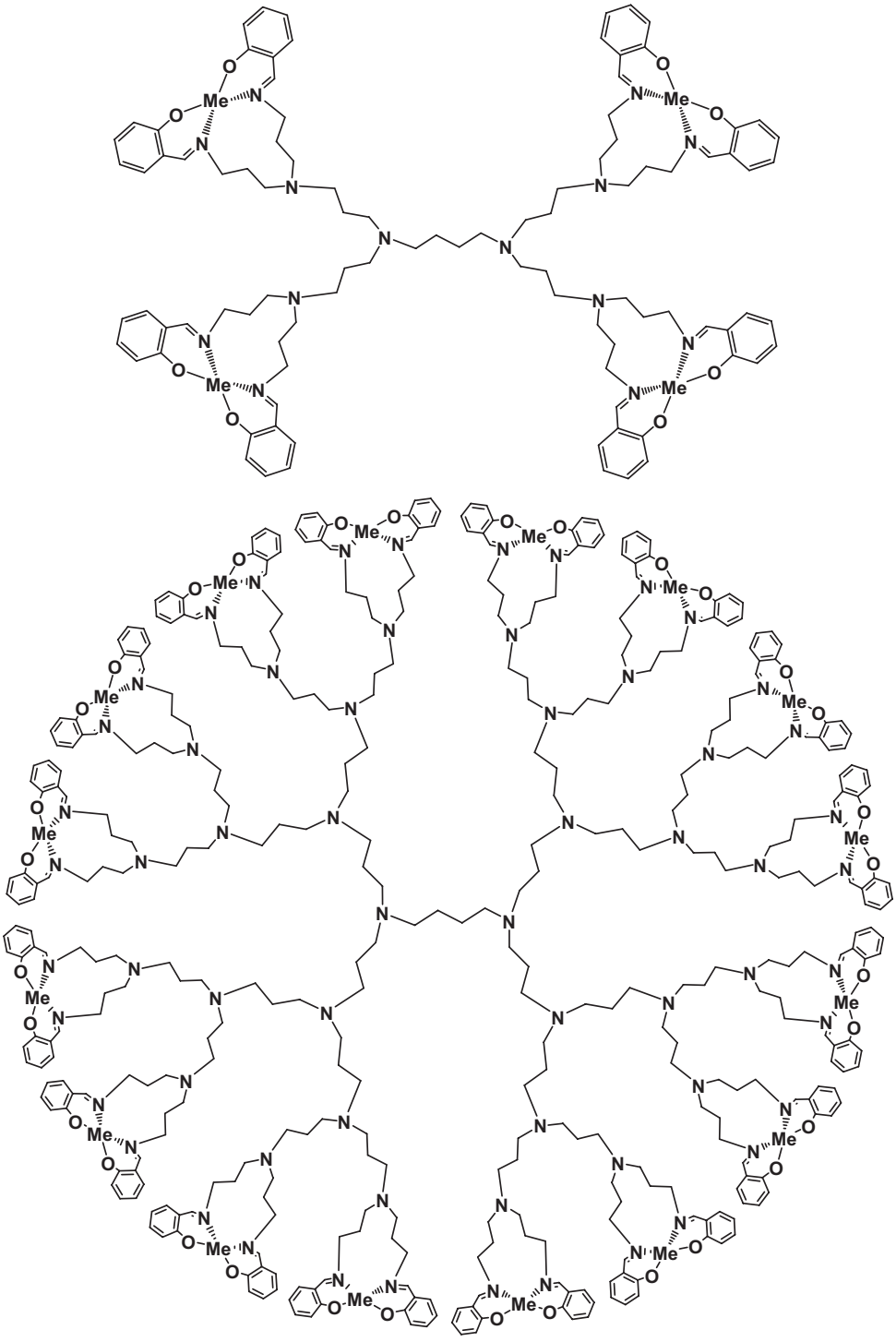

Scheme 3. (A) Generation 2 and (B) generation 4 metallo-functionalized salicylaldimine Lig1 dendrimers.

Solutions of different concentrations were freshly prepared before each experiment by dilution of the appropriate quantity in acetone and ethanol, molar ratio 1:1.

Microvolumes were measured using EP-10 and EP-100 Plus Motorized Microliter Pippettes (Rainin Instrument Co. Inc., Woburn, USA). The pH measurements were carried out with a Crison micropH 2001 pH-meter with an Ingold combined glass electrode. All experiments were done at room temperature ($25 \pm 1\,^{\circ}C$).

2.2. Preparation of first-generation salicylaldiamine ligands and metallo-functionalized dendrimers modified carbon electrode surfaces

Thin films of salicylaldiamine dendritic ligands, Lig1 and Lig2, and metallo-functionalized dendrimers, Co–Lig1, Co–Lig2, Cu–Lig1, Cu–Lig2, Ni–Lig2 [7], were deposited onto GCE for the electrochemical study and on HOPG for the MAC Mode AFM imaging.

Table 1
Supporting electrolytes, 0.1 M ionic strength

pH	Composition
2.2	HCl + KCl
3.3	HAcO + NaAcO
4.0	HAcO + NaAcO
5.0	HAcO + NaAcO
6.0	$NaH_2PO_4 + Na_2HPO_4$
7.0	$NaH_2PO_4 + Na_2HPO_4$
9.5	$NH_3 + NH_4Cl$
12.1	NaOH + KCl

Salicylaldiamine dendritic ligands or metallo-functionalized dendrimer solutions of different concentrations were prepared in a 50% mixture acetone/ethanol, and 8 μL were deposited onto HOPG or GC electrode surfaces and the solvent allowed to evaporate completely. The modified electrode surfaces were then washed with a jet of ethanol, followed by a jet of deionized water, in order to clean the excess of molecules loosely adsorbed on the surface. The modified carbon electrode was subsequently allowed to dry again in a sterile atmosphere at room temperature.

2.3. Atomic force microscopy

Highly oriented pyrolytic graphite (HOPG), grade ZYB of dimension 15 mm × 15 mm × 2 mm from Advanced Ceramics Co., was used as a substrate. The HOPG was freshly cleaved with adhesive tape prior to each experiment and imaged by MAC Mode AFM in order to establish its cleanliness.

AFM was performed with a PicoSPM equipment controlled by a MAC Mode module and interfaced with a PicoScan controller from Molecular Imaging Corp., Tempe, AZ. All the AFM experiments were performed with a CS AFM S scanner with a scan range 6 μm in *x*–*y* and 2 μm in *z*, from Molecular Imaging Corporation. Silicon type II MAClevers of 225 μm length, 2.8 N m^{-1} spring constants and 60–90 kHz resonant frequencies in air and 27–30 kHz resonant frequencies in liquid (Molecular Imaging Co.) were used. All images (256 samples/line × 256 lines) were taken at room temperature; scan rates 0.8–2.2 lines s^{-1}. When necessary, MAC Mode AFM images were processed by flattening in order to remove the background slope and the contrast and brightness were adjusted.

2.4. Voltammetric parameters and electrochemical cell

Voltammetric experiments were carried out using a μAutolab running with GPES 4.9 software, Eco-Chemie, Utrecht, The Netherlands. Measurements were carried out using a glassy carbon electrode (GCE) ($d = 2.0$ mm) as working electrode (Metrohm 6.1204.110), a Pt foil counter electrode (Metrohm 6.0305.100), and a Ag/AgCl (3 M KCl) as reference (Metrohm 6.0733.100), in a 20 ml one-compartment electrochemical cell. Differential pulse voltammetry (DPV) conditions were pulse amplitude 50 mV, pulse width 70 ms, scan rate 5 mV s^{-1}. Square wave voltammetry (SWV) conditions were frequency 25 Hz and potential increment 2 mV, corresponding to an effective scan rate of 50 mV s^{-1}.

The GCE was polished using diamond spray (particle size 6 μm) before each experiment. After polishing, the electrode was rinsed thoroughly with Milli-Q water for 30 s; then it was sonicated for 1 min in an ultrasound bath and again rinsed with water. After this mechanical treatment, the GCE was placed in buffer electrolyte and various voltammograms were recorded until a steady-state baseline voltammogram was obtained. This procedure ensured very reproducible experimental results.

2.5. Acquisition and presentation of voltammetric data

All the voltammograms presented were background subtracted and baseline corrected using the moving average with a step window of 5 mV included in GPES Version 4.9 software. This mathematical treatment improves the visualization and identification of peaks over the baseline without introducing any artifact, although the peak height is in some cases reduced (<10%) relative to that of the untreated curve. Nevertheless, this mathematical treatment of the original voltammograms was used in the presentation of all experimental voltammograms for a better and clearer identification of the peaks.

3. Results

3.1. Atomic force microscopy imaging

The first-generation salicylaldimine ligands and metallo-functionalized dendrimer modified carbon electrode surfaces, were prepared by adsorption onto the HOPG electrode. The two different substituted salicylaldiamine dendritic ligands and their complexes with cobalt, copper and nickel were morphologically characterized by MAC Mode AFM in air. The HOPG electrode was chosen as substrate for the AFM experiments, because the small, first-generation dendrimers can only be correctly imaged by AFM when they are attached onto very smooth electrode surfaces. For comparison, the GCE, used in electrochemical studies, has a root-mean-square (rms) roughness of 2.10 nm while the basal plane of the HOPG electrode has a rms roughness of less than 0.06 nm, for a 1000 nm × 1000 nm surface area. The electrochemical experiments using GCE and HOPG electrodes presented a similar behaviour.

The modification of the HOPG electrode was performed by placing a 8 μL drop of solutions of different concentrations of ligand or metal–ligand complexes on the HOPG surface, as described in Section 2.

The measured height of the ligands and metal complexes adsorbed onto the HOPG surface was always lower than their observed diameter. The dimensions of the dendrimers typically range from one to several nanometers, and they exhibit increasing sizes with increasing degree of molecular branching (generation) (Schemes 1–3).

The first-generation dendrimers used in this study are very small, and the geometric parameters of the AFM tip, with approximately 10 nm radius of curvature, represents a limiting factor in the high-resolution investigation. The larger full width at half-maximum height (fwhm) measured when compared with height, is due to the convolution effect of the AFM tip radius.

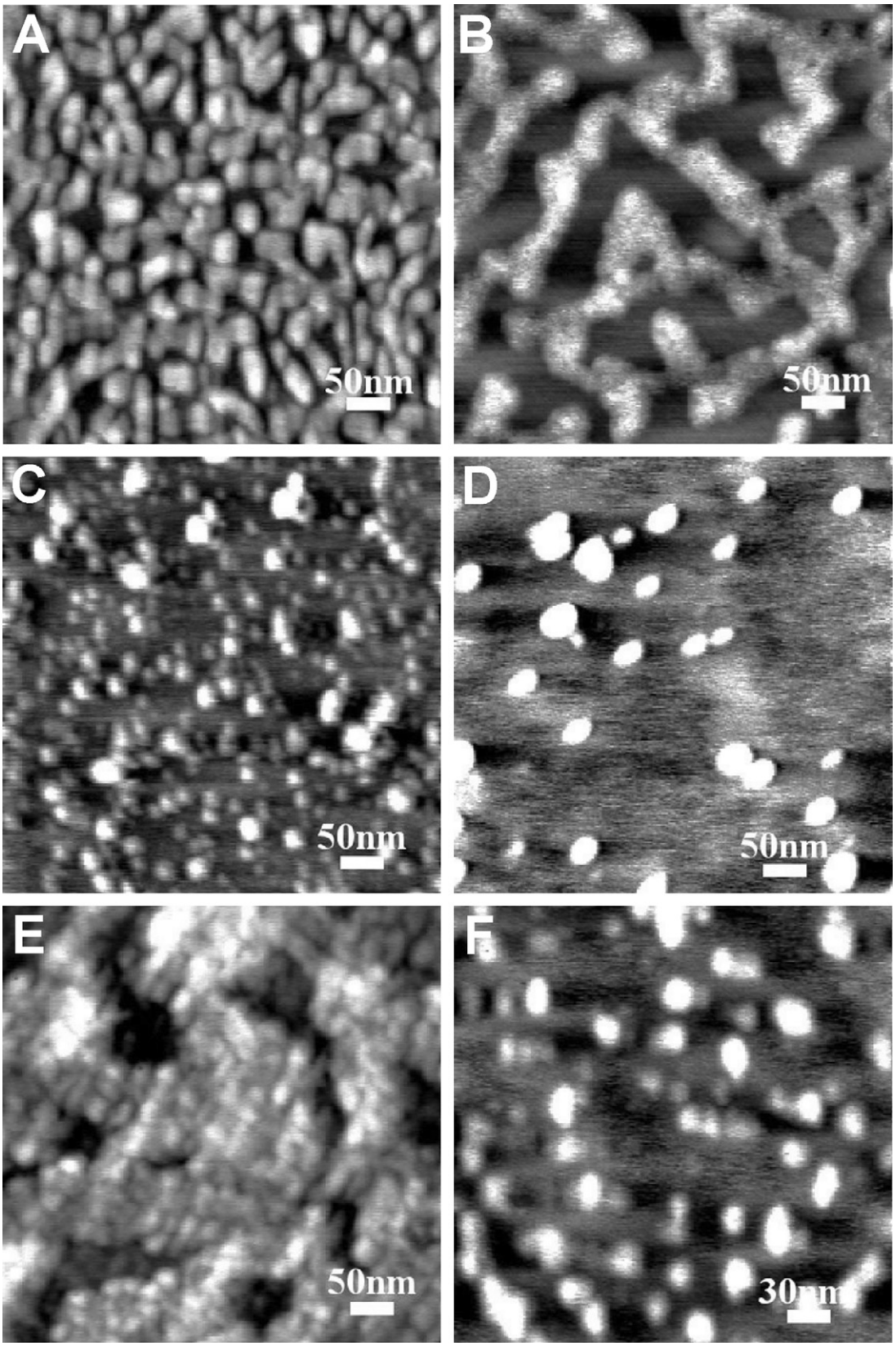

Fig. 1. MAC Mode AFM topographical images in air of HOPG modified by (A) 5.0 mM and (B) 1.0 mM salicylaldiamine Lig1; (C) 5.0 mM Cu–Lig1, (D) 5.0 mM Co–Lig1; (E) 5.0 mM Ni–Lig1 and (F) 2.5 mM Ni–Lig1 complexes.

Estimates of the AFM measured width of adsorbed molecules can be obtained using a simplified model of a parabolic or spherical tip in contact with a small, well-defined, incompressible, spherical molecule. In the case of an AFM tip with spherical geometry, the apparent width, l, of a molecule of radius r depends on the AFM tip radius R according to the formula: $l = \sqrt{Rr}$ [20], while for an AFM tip with a parabolic geometry and $R > r$, the apparent width is $l = 4(R + r)\sqrt{r(R - r)}/R$ [21]. Assuming a first-generation dendrimer as a sphere, for a tip radius of approximately 10 nm we expect that a single dendrimer will appear in the AFM images as a spherical aggregate, with an overestimated helix diameter and apparent length, due to the convolution effect of the radius of curvature of the AFM tip. Nevertheless, since the tip is responsible for such a big contribution to the measured width, it is not possible to distinguish between one and two molecules that condensate together.

On the other hand, during the sample scan, the AFM tip geometry has a dynamic behaviour due to the adsorption of sample onto the tip and breakage of small parts of the tip, incidents that can lead to an increase of the tip's radius of curvature. Additionally, the dendrimers are soft and easily deformed, which results in an increased fwhm of the adsorbed first-generation dendrimers observed in the images.

Compared with the fwhm measurements, the height give a better representation of the dendrimer diameter, since it is not limited by the tip's radius of curvature. For this reason, only height measurements were considered in all experiments described below.

The HOPG electrode modified by the two different substituted first-generation salicylaldimine dendritic ligands, Lig1 and Lig2, and metallo-functionalized dendrimers, Co–Lig1, Cu–Lig1, Ni–Lig1, and Co–Lig2, Cu–Lig2, was imaged for different solution concentrations.

3.1.1. Salicylaldiamine dendritic ligand 1

The HOPG electrode was modified by depositing Lig1 by evaporation from a 5.0 mM solution (Fig. 1A). The adsorbed molecules self-arranged in very compact networks that can be seen over the entire image, representing very compact individual dendrimer units, and covered the large HOPG area visualized in air by AFM. This very smooth monolayer film had only 0.91 nm rms roughness for a 500 nm × 500 nm surface area, Fig. 1A, and the measured thickness of the lattice presented uniform values and 2.8 ± 0.6 nm of height. The Lig1 molecules interact strongly with the HOPG electrode through hydrophobic interactions of the π-electron system of the aromatic rings of the Lig1 molecules with the HOPG hydrophobic surface.

In order to observe the internal morphological structure of the Lig1 film, adsorption from a less concentrated solution was also investigated. Adsorption from 2.5 mM Lig1 (data not shown) and 1.0 mM Lig1 solutions, Fig. 1B, led to incomplete films on the HOPG surface of 0.68 nm rms roughness, forming networks with parts of the HOPG surface still uncovered by Lig1 molecules. The small, closely packed Lig1 aggregates built network arms, which showed slightly smaller heights of 1.8 ± 0.2 nm.

3.1.2. Metallo-functionalized dendrimers, Me–Lig1

The investigation of the first-generation salicylaldimine Lig1–metal (Co, Cu and Ni) complexes proved to be a more complex situation and AFM images demonstrated that all metallo-functionalized dendrimers adsorbed strongly onto HOPG.

The Cu–Lig1 complexes were deposited by evaporation from a 5.0 mM solution concentration, and they appear in the AFM images as small spheres, with 0.9 ± 0.3 nm of height and 0.45 nm rms roughness for the 500 nm × 500 nm surface area (Fig. 1C).

The small Co–Lig1 complexes deposited by evaporation from a 5.0 mM solution concentration, also adsorbed on the HOPG electrode surface, Fig. 1D, but the HOPG electrode presented a smaller degree of surface coverage, demonstrating that Cu–Lig1, Fig. 1C, complexes interact strongly with the HOPG electrode when compared to Co–Lig1, Fig. 1D, for the same solution concentration. The adsorbed molecules appeared in the AFM image as globular nanoclusters with 2.4 ± 0.6 nm of height and the film had 0.46 nm rms roughness (Fig. 1D). The interaction between the molecules decreased and only a few larger nanoclusters of approximately 2 nm of height, formed by several molecules, were observed in the images.

The Ni–Lig1 complexes were deposited by evaporation from a 5.0 mM solution concentration and adsorbed much more strongly on the surface of the electrode than the other metal complexes (Fig. 1E). The molecules formed a granular film of 1.03 nm rms roughness and approximately 3.0–6.0 nm of height. To observe better the internal morphological structure of the Ni–Lig1 complex film, adsorption from a less concentrated solution was also investigated. The Ni–Lig1 complexes were deposited from a lower 2.5 mM solution concentration and the molecules appeared as very small globular aggregates, uniformly dispersed on the HOPG (Fig. 1F). The pattern of adsorption and the degree of surface coverage were similar to those obtained for the Cu–Lig1 complexes, Fig. 1C, with an average height and standard deviation of the spherical aggregates of 2.5 ± 0.6 nm. The rms roughness of an 500 nm × 500 nm image was 0.70 nm.

3.1.3. Salicylaldiamine dendritic ligand 2

The HOPG electrode was modified by depositing Lig2 by evaporation from a 5.0 mM solution concentration (Fig. 2A). The Lig2 presented a very weak adsorption on the HOPG surface, a very different result when compared with Lig1 molecules immobilised from the same solution concentration of 5.0 mM and identical experimental conditions. The Lig2 nanoclusters presented irregular shapes and sizes, although they were uniformly distributed over the whole HOPG surface. Measurements performed by section analysis in the images revealed a larger average height and a higher standard deviation of the particles of 3.5 ± 1.0 nm and the film had a 0.99 nm rms roughness (Fig. 2A).

The only structural difference between the two ligands, Scheme 1, is the presence of eight butyl groups on meta positions on the aromatic rings of the Lig2, that hinder the hydrophobic interactions between Lig2 and the HOPG surface.

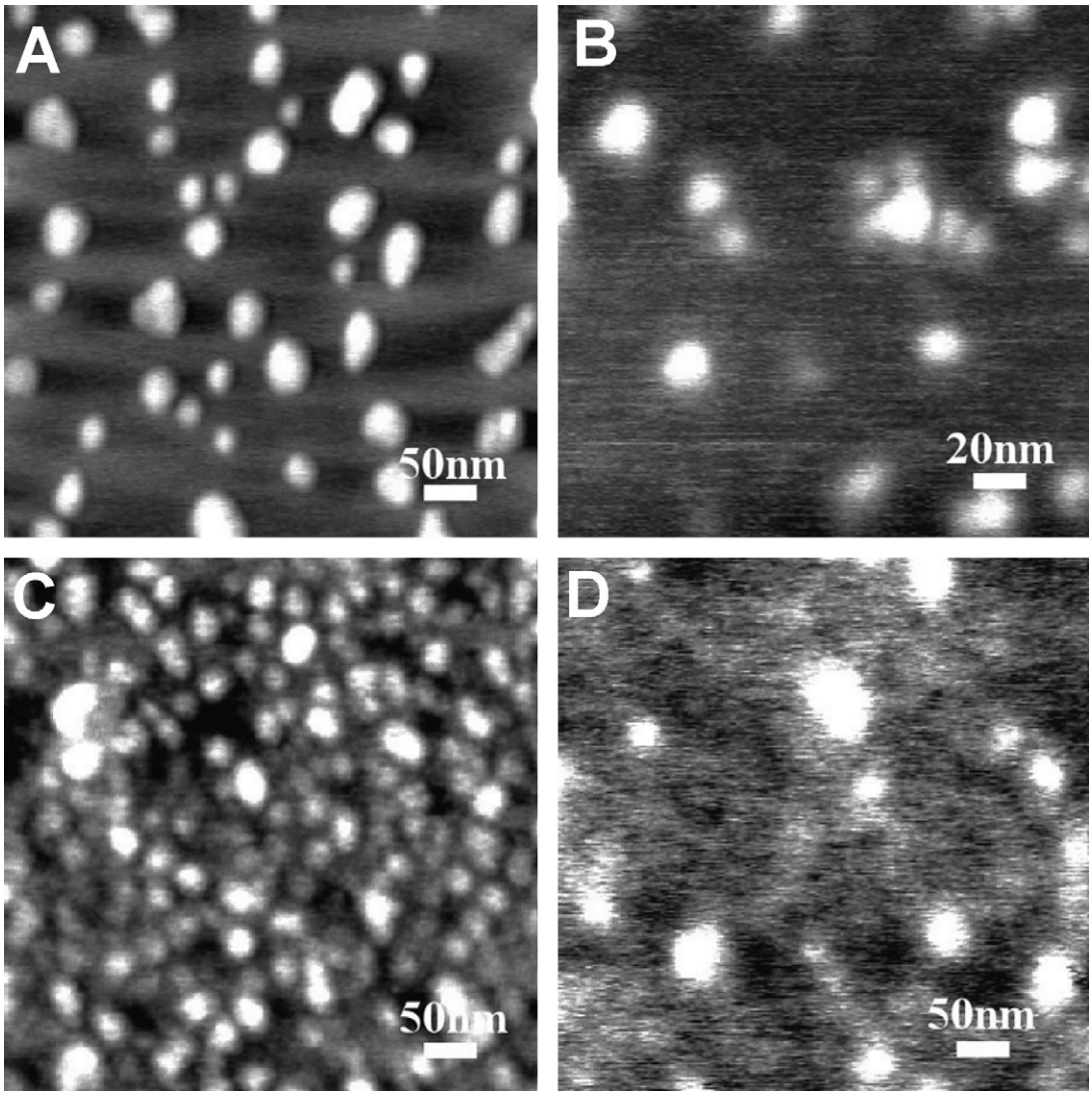

Fig. 2. MAC Mode AFM topographical images in air of HOPG modified by (A) 5.0 mM salicylaldiamine Lig2, (B) 5.0 mM Cu–Lig2, (C) 5.0 mM Co–Lig2, and (D) 2.5 mM Co–Lig2 complexes.

3.1.4. Metallo-functionalized dendrimers, Me–Lig2

The adsorption pattern of Cu–Lig2, deposited by evaporation from a 5.0 mM solution concentration, Fig. 2B, was similar to that observed for Cu–Lig1 complexes. On the surface of HOPG very small nanoclusters were observed, corresponding to the adsorption of groups of individual molecules on the HOPG. The nanoparticle height measured by AFM was of 1.8 ± 0.3 nm and the rms roughness of an 500 nm × 500 nm image was 0.60 nm.

The interaction of Co–Lig2 complexes with the surface of the HOPG electrode was initially investigated after deposition followed by evaporation from a solution of 5.0 mM concentration. A very thick film was observed on the HOPG surface of 0.45 nm rms roughness, Fig. 2C, formed by densely packed globular aggregates. In order to observe the internal morphological structure of the Co–Lig2 film, adsorption after deposition followed by evaporation from a 2.5 mM solution, was also investigated (Fig. 2D). Under this conditions the MAC Mode AFM images confirmed the existence of a number of isolated Co–Lig1 nanoparticles of diameter 2.1 ± 0.5 nm embedded into a smooth thin monolayer film with 0.37 nm rms roughness.

3.2. Electrochemical studies

The AFM topographic images showed clearly that the first-generation salicylaldimine ligands and metallo-functionalized dendrimers modified the HOPG electrode surfaces by adsorption, after deposition followed by solvent evaporation, from different solution concentrations.

Electrochemical characterization of the first-generation salicylaldimine ligands and metallo-functionalized dendrimers modified GCE surfaces was done by DPV and SWV. The electrode was modified using the same experimental conditions as in AFM. These GC electrodes modified by the surface-confined first-generation salicylaldimine ligands or metallo-functionalized dendrimers were immersed in 0.1 M ionic strength buffer solutions, over a wide pH range, between

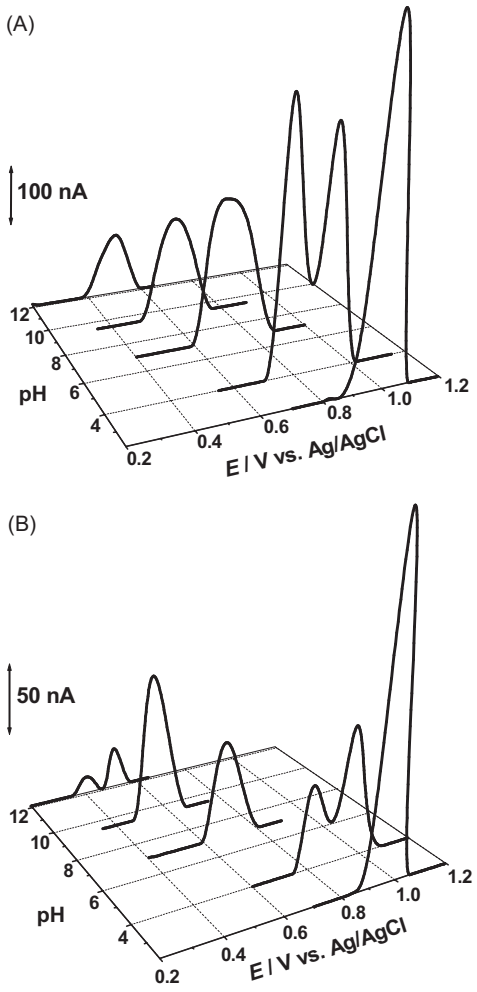

Fig. 3. 3D plot of first DPVs obtained in electrolytes with different pH values: (A) Lig1 and (B) Lig2 deposited by evaporation on the GCE surface. Scan rate = 5 mV s^{-1}.

2.2 and 12.1, Table 1, and voltammetric studies were done. This procedure has the advantage that all redox processes occurring are due to the surface-confined compound adsorbed on the GCE surface and ensures that there is no contribution of species diffusing from bulk solution.

3.2.1. Salicylaldiamine dendritic ligand 1

The electrochemical oxidation of Lig1 was studied by DPV, Fig. 3A, and showed that the Lig1 oxidation mechanism is complex and, depending on the pH, one or two consecutive charge transfer reactions were observed. The variation of peak potential, E_p, with pH is plotted for the different pH values studied (Fig. 5A).

For a very low pH only one oxidation peak P1 occurs and the width at half height, $W_{1/2} = 92$ mV suggests that the oxidation of Lig1 involves the transfer of one electron. Increasing the electrolyte pH, a new peak P2 occurred at lower potentials than peak P1. The width at half height for both peaks P1 and P2 was also $W_{1/2} \sim 90$ mV suggesting two consecutive charge transfer reactions, each one of them involving the transfer of one electron. For pH > 5, only one very broad peak, $W_{1/2} = 180$ mV, was observed suggesting that the charge transfer reaction was of a more complex nature involving two or more consecutive reactions that could not be clearly separated under the DPV conditions used. Nevertheless, Fig. 5A showed that the potential of both peaks is pH-dependent and the slope of the lines, 30 mV per pH unit, suggested that the number of protons transferred during Lig1 oxidation is half the number of electrons involved.

SWV was also employed to investigate the reversibility of the peaks already observed with DPV and the existence of oxidation products of the ligands. Although SW voltammograms were recorded for all compounds (ligands and their metal complexes) only the voltammograms obtained after deposition of Lig1 are presented since the other compounds showed a similar behaviour. The advantages of this technique are greater speed of analysis, lower consumption of the electroactive species in relation to DPV, and reduced problems with poisoning of the electrode surface.

On the first SWV scan obtained after deposition by evaporation of Lig1 onto the GCE surface only one broad peak occurred (Fig. 4A). However, a small shoulder, peak P2, could be distinguished on the rising current part of the voltammogram followed by peak P1 at a higher potential value. The forward and backward current components of the total current led to the conclusion that the oxidation of Lig1 is an irreversible two-step process.

During a second SWV recorded under the same conditions and immediately after the first scan a new peak occurred at a much lower potential value followed by peak P1 (Fig. 4B). This new peak corresponds to oxidation of the adsorbed Lig1 oxidation product on the GCE surface that was formed on the first SWV scan. The reversibility of this new peak was confirmed by plotting the forward and backward current components of the total current. The oxidation and the reduction currents are equal and the value of the potential of the forward and backward peaks is identical, corresponding to an adsorbed product of the Lig1 reversible oxidation process (Fig. 4B).

The electrochemical reduction of Lig1 was studied by SWV and showed in pH 7.0, buffer and only on the second scan, a reversible peak at ~−0.3 V (data not shown), corresponding to the reduction of a Lig1 oxidation product.

3.2.2. Metallo-functionalized dendrimers, Me–Lig1

The electrochemical oxidation of the first-generation salicylaldimine metallo-functionalized dendrimers, Me–Lig1, of copper, cobalt and nickel, was also investigated over the same pH range and under the same conditions of adsorption onto GCE.

The Cu–Lig1 complexes were deposited by evaporation of 8 μL from a 5.0 mM solution on the GCE surface. In the DPVs obtained, both peaks P1 and P2 were observed, Figs. 5B and 6, for a wide pH range, which did not happen with Lig1. For higher pH values only peak P2 remained. Nevertheless, Fig. 5B, shows that both peaks P1 and P2 are pH depended for pH < 5.0 and pH < 7.0, respectively, and the slope of the lines are 30 mV per pH unit, as found for Lig1. Peaks P1 and P2 were both observed, in the DPVs obtained in pH 4.0 0.1 M acetate buffer (Fig. 6A). The peak potentials are similar to those obtained for Lig1 oxidation but the currents are several times smaller. Both peaks occurred also on the DP voltammogram recorded in pH 7.0 0.1 M phosphate buffer, Fig. 6B, contrary to what was observed for the

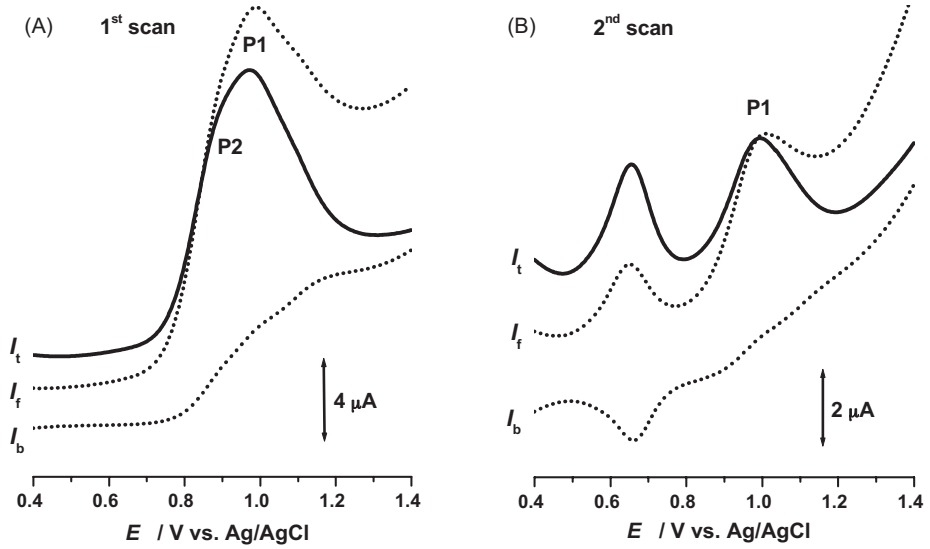

Fig. 4. SW voltammograms obtained in pH 4.0 0.1 M acetate buffer of Lig1 deposited on the GCE surface: (A) first scan and (B) second scan. $f = 25$ Hz, $\Delta E_s = 2$ mV, $v_{eff} = 50\ mV\ s^{-1}$, pulse amplitude 50 mV; I_t, total current, I_f, forward current, and I_b, backward current.

oxidation of Lig1, Fig. 5A, where under the same conditions only peak P2 was observed.

The oxidation of Co–Lig1 was also carried out over the same pH range, Figs. 5C and 6. The DPV obtained in pH 4.0 0.1 M acetate buffer showed peaks P1 and P2 at the same potential as those for Lig1 oxidation but again with much lower currents (Fig. 6A). On the other hand, in pH 7.0 0.1 M phosphate buffer besides peak P1 and P2 a new peak P3 occurred at high posi-

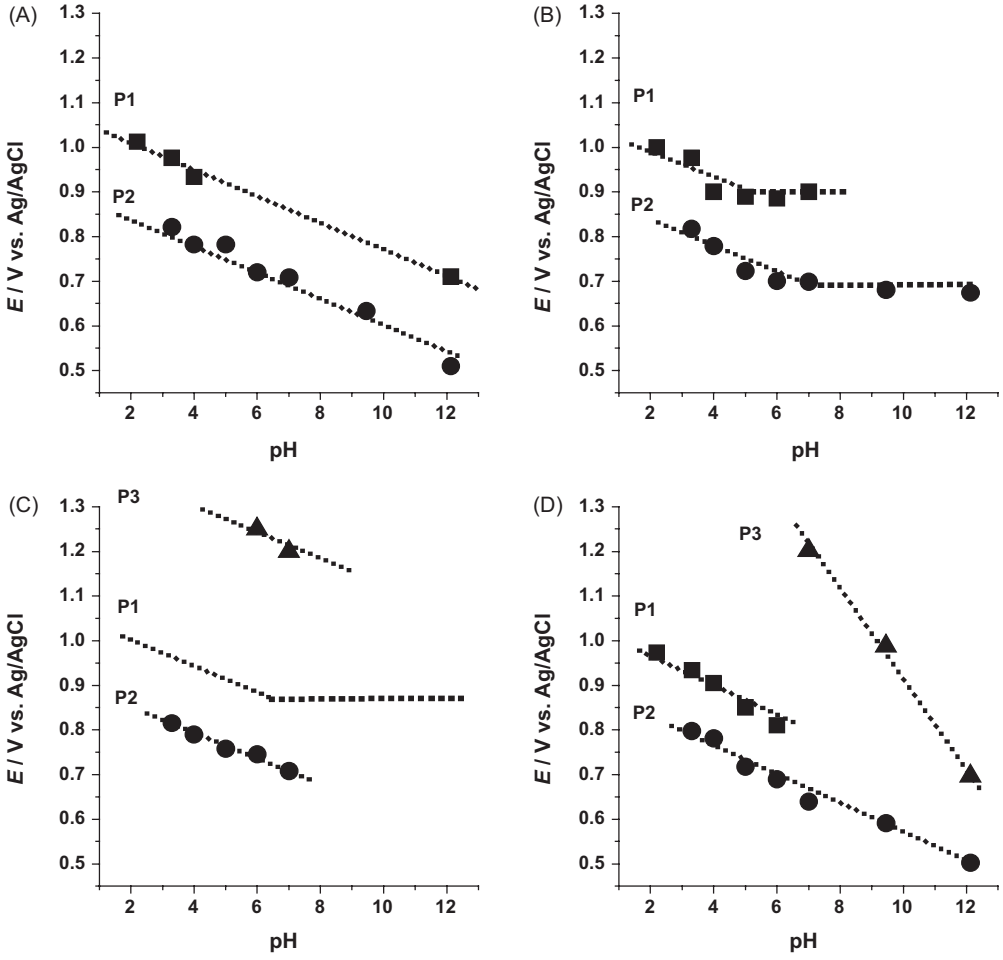

Fig. 5. Plots of peak potentials, E_{pa} of (A) Lig1, (B) Cu–Lig1, (C) Co–Lig1, and (D) Ni–Lig1 vs. pH, obtained by DPV for a wide pH range. Scan rate = 5 mV s^{-1}.

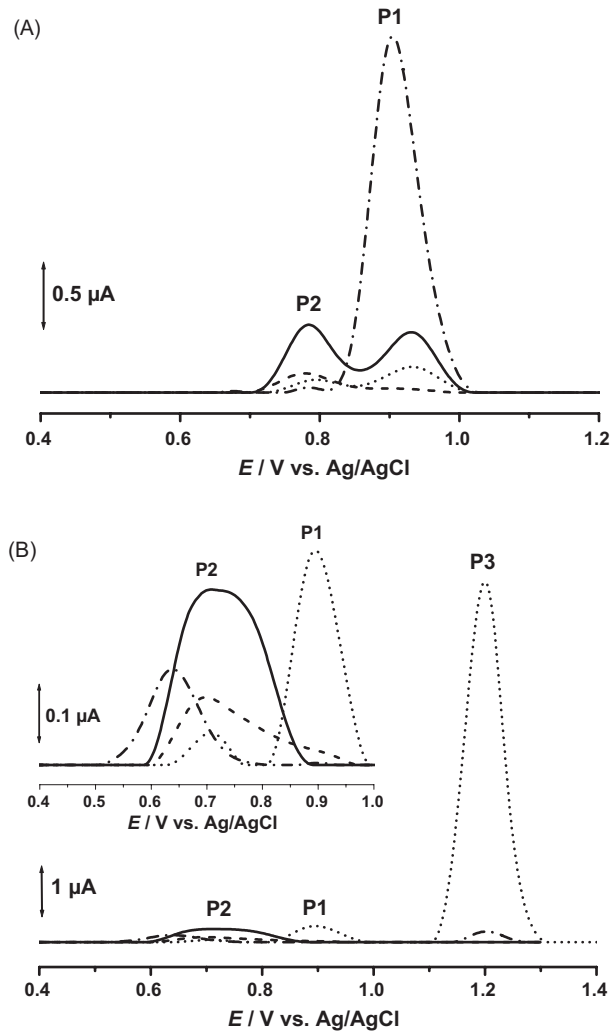

Fig. 6. Baseline-corrected DPVs after deposition on the GCE surface of (▬) Lig1, (▪▪▪) Cu–Lig1, (●●●) Co–Lig1 and (●▪●▪●) Ni–Lig1, in (A) pH 4.0 0.1 M acetate buffer and (B) pH 7.0 0.1 M phosphate buffer. Scan rate = 5 mV s^{-1}.

tive potentials, E_p = +1.20 V (Figs. 5C and 6B). This peak was observed only in phosphate buffers, 6.0 < pH < 7.0. It is important to mention that the DPV recorded in the same conditions but with a bare GCE surface even scanning to a much higher potential limit (+1.60 V) did not show any peak. Thus peak P3 is a clear indication of a new electron-transfer reaction. For pH < 7.0, peaks P1 and P2 are pH-dependent and the slope of the lines is 30 mV per pH unit. For higher pH values only peak P1 was observed and is pH-independent (Fig. 4C).

In the case of Ni–Lig1, the study was also carried out over the same pH range (Figs. 5D and 6). All peaks are pH-dependent, the slope of the lines for peaks P1 and P2 being 30 mV per pH unit while for peak P3 a relationship of 60 mV per pH unit was observed after fitting the data (Fig. 5D). Peak P1 and P2 both appeared in the DPV obtained in pH 4.0 0.1 M acetate buffer (Fig. 6A). Although peak P1 presented a very low current, peak P2 current increased significantly when compared with peak P2 current obtained for the oxidation of Lig1 alone. In pH 7.0 0.1 M phosphate buffer peak P2 still occurred whereas P1 virtually disappeared but a new peak P3 was observed, at higher positive potentials, as occurred for Co–Lig1 (Fig. 6B).

SWV was also employed to investigate the reversibility of the peaks observed with DPV and the existence of oxidation products of all the metallo-functionalized Lig1 dendrimers (data not shown). They all showed a similar behaviour corresponding to the oxidation of the ligand and adsorbed ligand oxidation products.

3.2.3. Salicylaldiamine dendritic ligand 2

The electrochemical oxidation of Lig2 deposited by evaporation onto the GCE surface was also investigated for different pH values using DPV (Figs. 3B and 7A). The main oxidation peak P2 was observed over the whole pH range whereas peak P1 occurred only at pH 4.0 and pH 12.1. The peak P2 potential was displaced to less positive values with increasing pH of the supporting electrolyte, showing a linear relationship of slope 60 mV per pH unit which corresponds to a redox mechanism that involves the same number of electrons and protons (Fig. 7A). Taking into consideration that the peak width at half height was $W_{1/2}$ = 100 mV in all electrolytes, it can be concluded that the oxidation of Lig2 occurred with the transfer of one electron and one proton.

SWV was also employed and showed similar ligand oxidation behaviour as DPV, as well as reversible oxidation of the ligand adsorbed oxidation products. The electrochemical reduction of Lig2, studied by SWV, showed in pH 7.0, only on the second scan, like Lig1, a reversible peak at −0.20 V (data not shown), corresponding to the reduction of the Lig2 oxidation product.

3.2.4. Metallo-functionalized dendrimers, Me–Lig2

The electrochemical oxidation of the first-generation salicylaldimine metallo-functionalized dendrimers, Me–Lig1, of copper, and cobalt, was also investigated over the same pH range and under the same conditions.

The Cu–Lig2 complexes were deposited by evaporation from a 5.0 mM solution onto the GCE. Oxidation occurs in a one step mechanism (Fig. 7B and 8). The DPV obtained in pH 4.0 0.1 M acetate buffer, Fig. 8A, showed only one oxidation peak occurring at the same potential as peak P2 of Lig2. A similar behaviour was observed in pH 7.0 0.1 M phosphate buffer although a small shift to less positive potentials in the oxidation of Cu–Lig2 relative to Lig2 was observed (Fig. 8B). For pH < 9.5, the oxidation of Cu–Lig2 is pH-dependent, and the relationship is linear with a slope of 60 mV per pH unit (Fig. 7B). The width at half height of the oxidation peak of Cu–Lig2 is about 90 mV for all electrolytes corresponding to the transfer of one electron. For pH > 9.5, the peak potential does not depend on the electrolyte pH showing that in these cases the oxidation of Cu–Lig2 involves only the electron-transfer reaction (Fig. 7B).

The oxidation of Co–Lig2 was also carried out over the same pH range, Figs. 7C and 8, and the results obtained are quite similar to those of Co–Lig1, except that the slope of the lines for Co–Lig2 is 60 mV per pH unit (Fig. 7C). Concerning Co–Lig2 oxidation, the DPV obtained in pH 4.0 0.1 M acetate buffer presented two main oxidation peaks similarly to Lig2, Fig. 8A, but although peak P2 occurred at the same potential as in

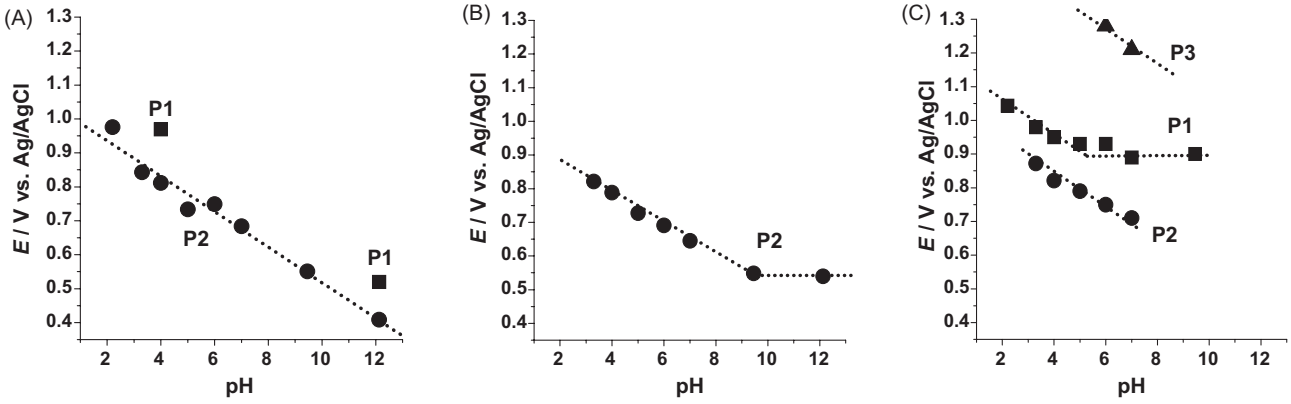

Fig. 7. Plots of peak potentials, E_{pa}, of (A) Lig2, (B) Cu–Lig2 and (C) Co–Lig2 vs. pH, obtained by DPV for a wide pH range. Scan rate = 5 mV s^{-1}.

the case of Lig2, peak P1 appeared at a more positive value. Nevertheless, a small shoulder could be observed following peak P2. On the other hand, in pH 7.0 0.1 M phosphate buffer peak P2 occurred at more positive potentials when compared with Lig2 oxidation, and two new peaks P1 and P3 were observed at a higher positive potential (Figs. 7C and 8B). For pH < 7.0 peaks P1 and P2 are pH-dependent and for higher pH values, only peak P1 was observed and became pH-independent, Fig. 7C, showing that the oxidation of Co–Lig2 at high pH involves only transfer of electrons. It is also important to notice that peak P3 again was only observed in phosphate buffers, 6.0 < pH < 7.0.

In the same way as for Lig2, SWV was also employed to check the reversibility of the peaks observed with DPV and the existence of oxidation products of all the metallo-functionalized Lig2 dendrimers (data not shown). They all demonstrated a similar behaviour corresponding to the oxidation of the ligand and adsorbed ligand oxidation products.

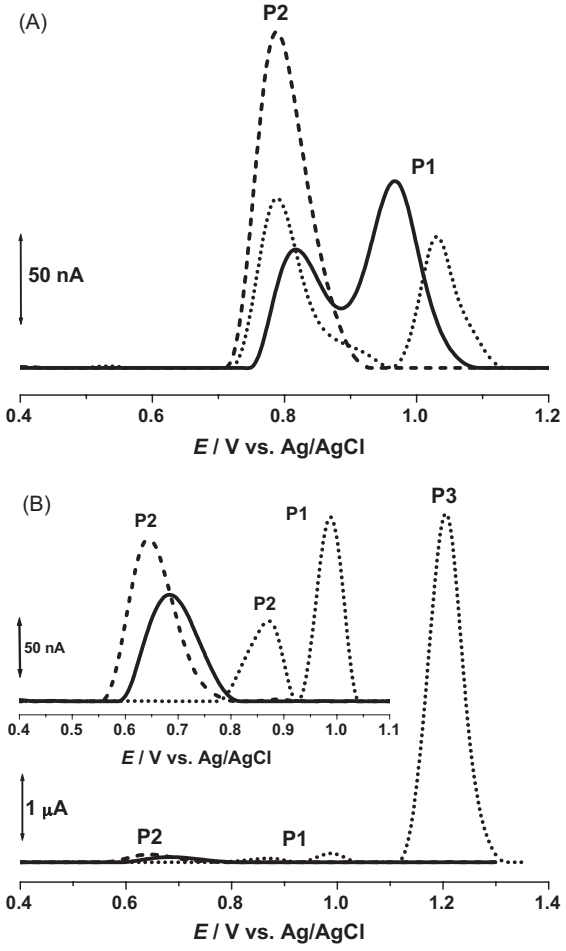

Fig. 8. Baseline-corrected DPVs after deposition on the GCE surface of (▬) Lig2, (▪▪▪) Cu–Lig2 and (●●●) Co–Lig2, in (A) pH 4.0 0.1 M acetate buffer and (B) pH 7.0 0.1 M phosphate buffer. Scan rate = 5 mV s^{-1}.

4. Discussion

First-generation salicylaldimine ligands and their cobalt, copper and nickel metallo-functionalized dendrimers were study for the first time by electrochemistry and MAC Mode AFM imaging. The dendrimers were immobilised by deposition followed by evaporation onto HOPG and GC electrodes from solutions of different concentrations.

The AFM results demonstrated that all the salicylaldimine ligands and their metallo-functionalized dendrimers adsorb on the surface of the HOPG electrode, resulting in the formation of generally spherical nanoclusters and films, and that the solvent evaporation dewetting process also affect the morphology of the films. Lig1 molecules present a very strong adsorption on the HOPG surface, when compared with Lig2 molecules immobilised from the same experimental and solution concentration conditions. The presence at the extremity of the Lig2 of eight additional butyl groups makes the occurrence of hydrophobic interactions between the aromatic rings of the molecule and the HOPG surface more difficult.

The electrochemical behaviour of both ligands is similar with only differences in the peak currents. Both salicylaldiamine dendritic ligands undergo oxidation at GCEs and the anodic currents for the oxidation of Lig1 are always higher than those observed for Lig2. Their redox mechanism is of a complex nature, depending on the pH of the supporting electrolyte and occurs in a cascade reaction. The anodic reactions correspond to the oxidation of the hydroxyl group electroactive centers that both ligands present in their structure. Since all experiments were car-

ried out with the ligands deposited by evaporation on the GCE surface and no diffusing species present in the supporting electrolyte, the differences in the oxidation peaks for both ligands are attributed to the presence of butyl groups on Lig2. As previously found by MAC Mode AFM, the interaction between the ligands and the GCE surface occurs in such a way that the Lig1 electroactive sites are able to be in direct contact with the electrode surface and can easily be oxidized. On the other hand, the presence of the eight butyl groups in Lig2 does not allow such a high flexibility, hindering the access to the electrode surface for oxidation of all the hydroxyl groups.

Nevertheless, it was shown that the oxidation of both ligands involves the transfer of one electron. However, the number of protons transferred during the electrochemical oxidation of Lig1 is half the number of electrons whereas the oxidation of Lig2 occurred with the transfer of the same number of electrons and protons. On the other hand, by using SWV it was shown that both ligands' redox reaction is an irreversible process that occurred with the formation of an electroactive species that is adsorbed on the electrode surface and undergoes reversible oxidation and reduction reactions.

The interaction with all the metal atoms causes destabilization of the internal structure of the two salicylaldiamine dendritic ligand molecules. Depending on the type of metal, copper, cobalt or nickel, incorporated on the first-generation metallo-functionalized dendrimers structure, the interaction of the hydrophobic π rings of the Lig1 and Lig2 molecules with the HOPG surface is decreased or increased.

The adsorption pattern of Cu–Lig1 molecules is similar to that of Cu–Lig2 complexes, proving the formation of more closely packed structures than those of the Lig1. The incorporation of Co in the structure of the salicylaldiamine dendritic Lig1 leads to a decrease of the surface coverage, due to the formation of a Co–Lig1 metallo-functionalized dendrimer more compact morphology. However, Co–Lig2 adsorbs more strongly on the surface of HOPG, when compared with the corresponding Lig2. The Ni–Lig1 complexes present a very strong adsorption on the HOPG surface, the same as observed for Lig1.

The electrochemical investigation of the first-generation salicylaldimine metallo-functionalized dendrimers also confirmed that destabilization of the ligand internal structure occurred. The peaks obtained during the electrochemical oxidation of these metallo-functionalized dendrimers are also due to the oxidation of hydroxyl groups, but the destabilization effect causes different accessibility of the ligand –OH groups on the GCE surface. This leads to the occurrence of peaks at different potentials when compared to the peaks obtained for the oxidation of the first-generation salicylaldimine ligands, the oxidation being always pH-dependent, as expected.

5. Conclusions

The voltammetric experiments and *ex situ* AFM demonstrated that first-generation dendritic ligands and metallo-functionalized dendrimers are electroactive and that spherical nanoclusters and films can be successfully immobilised at the surface of carbon electrodes. The morphological characteristics of the immobilised molecules and films, such as the structure, shape, and size are directly influenced by the type of metal incorporated into the structure and by the concentration of the solution used for deposition. The redox mechanism is complex, depends on the pH of the supporting electrolyte, and occurs in a cascade reaction. The electrochemical oxidation of these ligands is an irreversible process and involves the formation of an electroactive product that undergoes reversible oxidation and reduction. The incorporation of a metal into the salicylaldiamine dendritic ligand leads to destabilization effects of the internal structure and different accessibility of the electroactive centres to the electrode surface, depending on the type of metal.

Acknowledgements

Financial support from Fundação para a Ciência e Tecnologia (FCT), Post-Doctoral Grants SFRH/BPD/36110/2007 (V.C. Diculescu.), SFRH/BPD/27087/2006 (A.M. Chiorcea-Paquim), Project PTDC/QUI/65255/2006, POCI 2010 (co-financed by the European Community Fund FEDER), ICEMS (Research Unit 103), and National Research Foundation (NRF) of South Africa, is gratefully acknowledged.

References

[1] A.-M. Caminade, R. Laurent, J.-P. Majoral, Adv. Drug Deliver. Rev. 57 (2005) 2130.
[2] D.K. Smith, A.R. Hirst, C.S. Love, J.G. Hardy, S.V. Brignell, B. Huang, Prog. Polym. Sci. 30 (2005) 220.
[3] D. Méry, D. Astruc, Coordin. Chem. Rev. 250 (2006) 1965.
[4] C. Wang, M.R. Bryce, A.S. Batsanov, L.M. Goldberg, J.A.K. Howard, J. Mater. Chem. 7 (1997) 1189.
[5] B. Gonzalez, C.M. Casado, B. Alonso, I. Cuadrado, M. Moran, Y. Wang, A.E. Kaifer, Chem. Commun. 23 (1998) 2569.
[6] G.R. Newkome, Z. Yao, G.R. Baker, V.K. Gupta, P.S. Russo, M.J. Saunders, J. Am. Chem. Soc. 108 (1986) 849.
[7] G. Smith, R. Chen, S. Mapolie, J. Organomet. Chem. 673 (2003) 111.
[8] A. Berduque, M.D. Scanlon, C.J. Collins, D.W.M. Arrigan, Langmuir 23 (2007) 7356.
[9] B. Helms, J.M.J. Fréchet, Adv. Synth. Catal. 384 (2006) 1125.
[10] K. Inoue, Prog. Polym. Sci. 25 (2000) 453.
[11] M.F. Ottaviani, S. Bossmann, N.J. Turro, D.A. Tomalia, J. Am. Chem. Soc. 116 (1994) 661.
[12] M.F. Ottaviani, F. Montalti, N.J. Turro, D.A. Tomalia, J. Phys. Chem. B 101 (1997) 158.
[13] K. Takada, G.D. Storrier, J.I. Goldsmith, H.D. Abruña, J. Phys. Chem. B 105 (2001) 2404.
[14] D.J. Diaz, S. Bernhard, G.D. Storrier, H.D. Abruña, J. Phys. Chem. B 105 (2001) 8746.
[15] K. Takada, D.J. Diaz, H.D. Abruña, I. Cuadrado, B. González, C.M. Casado, B. Alonso, M. Morán, J. Losada, Chem. Eur. 7 (2001) 1109.
[16] H.D. Abruña, Anal. Chem. 76 (2004) 310A.
[17] V.V. Tsukruk, Adv. Mater. 10 (1998) 253.
[18] T. Gao, E.S. Tillman, N.S. Lewis, Chem. Mater. 17 (2005) 2904.
[19] C.A. Nijhuis, B.A. Boukamp, B.J. Ravoo, J. Huskens, D.N. Reinhoudt, J. Phys. Chem. C 111 (2007) 9799.
[20] F. Zenhausern, M. Adrian, R. Emch, M. Taborelli, M. Jobin, P. Descouts, Ultramicroscopy 42–44 (1992) 1168.
[21] C. Bustamante, J. Vesenka, C.L. Tang, W. Rees, M. Guthold, R. Keller, Biochemistry 31 (1992) 22.